Vol. 739: 129–146, 2024
https://doi.org/10.3354/meps14602

MARINE ECOLOGY PROGRESS SERIES
Mar Ecol Prog Ser

Published July 4

Temperature-dependent hypoxia tolerance of purple sea urchin *Strongylocentrotus purpuratus* across biogeography and ontogeny

Murray I. Duncan[1,2,3,4,5,*], Fiorenza Micheli[2,6], J. Andres Marquez[1], Christopher J. Lowe[7], Scott L. Hamilton[8], Erik A. Sperling[1]

[1]Earth and Planetary Science, Stanford University, Stanford, CA 94305, USA
[2]Oceans Department, Hopkins Marine Station, Stanford University, Pacific Grove, CA 93950, USA
[3]Department of Environment, University of Seychelles, Anse Royale 0000, Seychelles
[4]Blue Economy Research Institute, University of Seychelles, Anse Royale 0000, Seychelles
[5]Department of Ichthyology and Fisheries Science, Rhodes University, Makhanda 6139, South Africa
[6]Stanford Center for Ocean Solutions, Pacific Grove, CA 93950, USA
[7]Biology Department, Hopkins Marine Station, Stanford University, Pacific Grove, CA 93950, USA
[8]Moss Landing Marine Laboratories, San Jose State University, San Jose, CA 95039, USA

ABSTRACT: Ocean warming is increasing organismal oxygen demand, yet at the same time the ocean's oxygen supply is decreasing. For a patch of habitat to remain viable, there must be a minimum level of environmental oxygen available for an organism to fuel its metabolic demand — quantified as its critical oxygen partial pressure (pO_{2crit}). The temperature-dependence of pO_{2crit} sets an absolute lower boundary on aerobically viable ocean space for a species, yet whether certain life stages or geographically distant populations differ in their temperature-dependent hypoxia tolerance remains largely unknown. To address these questions, we used the purple sea urchin *Strongylocentrotus purpuratus* as a model species and measured pO_{2crit} for 3 populations of adult urchins (Clallam Bay, WA [n = 39], Monterey Bay, CA [91], San Diego, CA [34]) spanning 5–22°C and for key embryonic and larval developmental phases (blastula [n = 11], gastrula [21], prism [31], early-pluteus [21], late-pluteus [14], settled [12]) at temperatures of 10–19°C. We found that temperature-dependent hypoxia tolerance is consistent among adult populations exposed to different temperature and oxygen regimes, despite variable basal oxygen demands, suggesting differential capacity to provision oxygen. Moreover, we did not detect evidence for a hypoxia tolerance bottleneck for any developmental phase. Earlier larval phases are associated with higher hypoxia tolerance and greater temperature sensitivity, while this pattern shifts towards lower hypoxia tolerance and reduced temperature sensitivity as larvae develop. Our results indicate that, at least for *S. purpuratus,* models quantifying aerobically viable habitat based on pO_{2crit}–temperature relationships from a single adult population will conservatively estimate viable habitat.

KEY WORDS: Hypoxia tolerance · Deoxygenation · *Strongylocentrotus purpuratus* · Purple sea urchin · Warming threshold · Climate change

1. INTRODUCTION

The ocean is rapidly warming and losing oxygen, with direct consequences for biodiversity (Poloczanska et al. 2013, Breitburg et al. 2018, Frölicher et al. 2018). Recent meta-analyses highlight the disproportionate role hypoxia plays in driving negative performance responses of aquatic organisms (Sampaio et al. 2021) and the synergistic negative effects that occur when warming and hypoxia are considered together (Reddin

*Corresponding author: murray.duncan@unisey.ac.sc

et al. 2020). However, not all species and areas will be negatively affected (Fulton 2011, Audzijonyte et al. 2020, Lavender et al. 2021). These variable species- and place-specific responses will be determined in part by capacities to maintain physiological functioning as environmental conditions change (Somero 2010, Seebacher et al. 2015). As such, quantifying temperature and oxygen thresholds of vital physiological processes can serve as a useful gauge for predicting how species will respond as climate change intensifies (Bozinovic & Pörtner 2015, Madliger et al. 2017).

Physiological measurements related to aerobic metabolism are particularly important in an ocean that is warming and losing oxygen. Aerobic metabolism fuels the processes that sustain most life (Schulte 2015), and rates of aerobic metabolism are also fundamentally determined by environmental temperature and oxygen availability (Claireaux & Chabot 2016). The point where environmental oxygen becomes limiting for an organism's aerobic metabolism is its hypoxia threshold, a useful indicator of tolerance for low oxygen conditions, with a low value corresponding to a high hypoxia tolerance (Ultsch & Regan 2019). In the present study, we estimated hypoxia tolerance for adults as the critical oxygen partial pressure for standard metabolic rate (pO_{2crit}) — the lowest oxygen level at which an organism can maintain levels of aerobic metabolism required to simply survive (Ultsch & Regan 2019, Seibel et al. 2021). While the interpretation of pO_{2crit} as a measure of short-term hypoxia tolerance is debated (Wood 2018), benchmarking this trait against basal levels of aerobic metabolism sets an absolute lower boundary on viable oxygen levels, although ultimately an organism will need higher oxygen levels to fuel a sustainable metabolic level on ecological timescales (Regan et al. 2019, Deutsch et al. 2020, Seibel et al. 2021). pO_{2crit} varies significantly with temperature for most species (Rogers et al. 2016). At warmer temperatures, an organism requires more oxygen to fuel an elevated metabolism, which can result in a relatively higher pO_{2crit} — i.e. lower hypoxia tolerance, if oxygen supply does not keep pace (Borowiec et al. 2016). The temperature-dependence of a species' hypoxia tolerance is thus a critical physiological threshold through which one can infer responses to simultaneous ocean warming and deoxygenation (e.g. Fig. 1) (Sørensen et al. 2014).

Modeling the temperature-dependance of pO_{2crit} allows one to map this physiological threshold across the entire range of temperature and oxygen values that organisms are exposed to in the ocean (Fig. 1). From this relationship, one can then infer which species and in what areas warming and deoxygenation may exceed this physiological threshold (Somero 2010, Roman et al. 2019). For example, Chu & Gale (2017) reported that species-specific hypoxia tolerances of 3 indicator species (spot prawn, slender sole, and squat lobster) determine the extent of their spatial distributions into deoxygenated waters of the northeast Pacific Ocean and the magnitude of distributional shifts expected in response to seasonal hypoxic zone expansion. Temperature-dependent

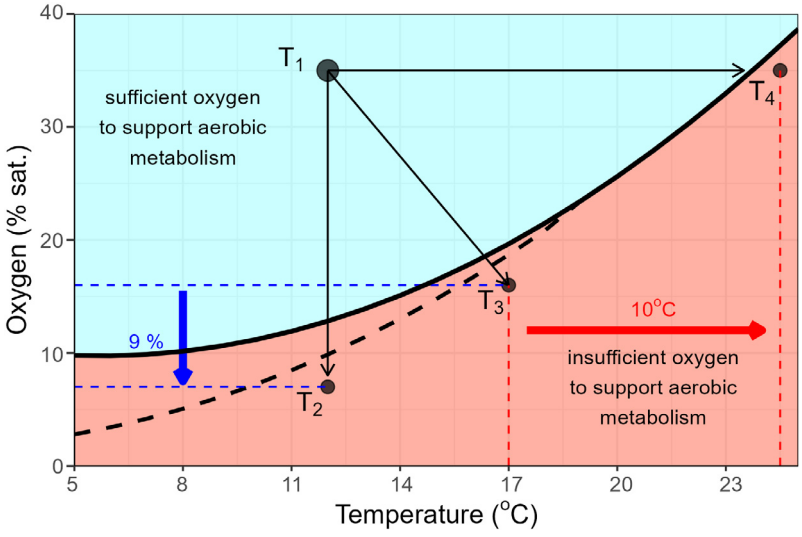

Fig. 1. Conceptual diagram of temperature-dependent hypoxia tolerance (pO_{2crit}, % air saturation, solid black line) delineating the ocean's temperature–oxygen space into conditions that can support aerobic metabolism (blue area) and conditions that cannot (red area). This pO_{2crit} model was obtained from measurements on *Strongylocentrotus purpuratus* from within Monterey Bay, CA (USA), in Duncan et al. (2023). Rising temperatures increase pO_{2crit} exponentially because organismal metabolic oxygen demand increases faster than supply, but this exponential pattern can break down at colder temperatures when oxygen is harder to obtain in more viscous water and pO_{2crit} is slightly higher than would be predicted by metabolic oxygen demand alone (black dashed line). Climate change can shift conditions from an initial climate state (T_1) to conditions that cannot support basal metabolic functioning via 3 pathways: T_2 (deoxygenation only), T_3 (deoxygenation and warming), or T_4 (warming only). Depending on the initial climate state, when warming and deoxygenation occur simultaneously, a relatively smaller absolute change in each environmental condition can result in an organism's hypoxia threshold being crossed. Whether the temperature-dependent hypoxia tolerance of a species is fixed or plastic, and whether it has a stage of development with particularly poor hypoxia tolerance, will in part determine its response to a warmer and deoxygenated future ocean

hypoxia tolerance is also used to calibrate species-specific parameters of the metabolic index (Deutsch et al. 2015) — a model that integrates ocean temperature and oxygen availability into a metric representing aerobic metabolic capacity. Indeed, the metabolic index has proven effective at explaining spatial variability in extinction rates across the Permian Triassic boundary (Penn et al. 2018), contemporary species biogeography (Deutsch et al. 2020, Duncan et al. 2020, 2023), and interannual variation in marine fish productivity (Howard et al. 2020b).

Despite the demonstrably useful information contained within measurements of pO_{2crit} (Regan et al. 2019) and how this trait changes with temperature, there is a dearth of intra-specific information available to understand how hypoxia tolerance changes with ontogeny or among geographically separated populations (Seibel & Deutsch 2020). The most recent compilations of studies where various hypoxia tolerance metrics (pO_{2crit}, oxygen level at 50% mortality [LD_{50}], oxygen level at loss of equilibrium [LOE]) are measured across 2 or more temperatures are found in Deutsch et al. (2020) and Rogers et al. (2016) for 80 aquatic species. However, of these 80 species, only 15 include measurements at 4 or more temperatures, all make hypoxia tolerance measurements of specimens from a single location, and only 1 study (on Atlantic rock crab *Cancer irroratus*, Vargo & Sastry 1977) measured hypoxia tolerance at any stage of development other than fully developed adults/juveniles. While there are studies on how hypoxia tolerance changes for a single early developmental stage across 2 temperatures (Rosa et al. 2013) or across multiple early developmental stages at a single temperature (Alter et al. 2015), we currently know very little regarding whether hypoxia tolerance changes over critical development phases across a wide range of temperatures, or if this threshold can change due to acclimation to variable environmental temperature and oxygen regimes, 2 characteristics that can significantly modulate climate responses.

The environmental conditions a species can tolerate can vary over development, with some phases (e.g. embryos, larvae) being particularly sensitive to temperature or hypoxia extremes, because they have energetically expensive developmental transitions and lack the capacity to regulate oxygen provision (Vaquer-Sunyer & Duarte 2008, Dahlke et al. 2020). Low tolerance to environmental variability during early development can result in a critical bottleneck for populations. If environmental conditions exceed the tolerance thresholds of a critical developmental phase, it can result in recruitment collapse and large declines in abundance and persistence (Rijnsdorp et al. 2009). Consequently, the response of a species to climate change will be determined by its most vulnerable developmental phase (Martin et al. 2020). Plasticity and local adaptability of these tolerance thresholds may dampen responses to variable and extreme environmental conditions, thus conferring enhanced climate resilience (Donelson et al. 2019). Following prolonged exposure to novel environmental conditions, the tolerance threshold of an organism can shift in the direction of this change, and initial acute responses to environmental variability may become dampened (Sinclair et al. 2016, Leung et al. 2021). The current knowledge gap around population-level and developmental variability in temperature-dependent hypoxia tolerance obfuscates predictions of how warming and deoxygenation may interact to drive a species' response to climate change.

To address this gap, we used the purple sea urchin *Strongylocentrotus purpuratus* as a model species in this study to provide a comprehensive assessment of intraspecific variability in temperature-dependent hypoxia tolerance over embryonic, larval, and settled developmental phases and from multiple adult populations exposed to different environmental temperature and oxygen regimes (Fig. 2). We predicted that temperature-dependent hypoxia tolerance varies across life stages, with early developmental phases being most sensitive to oxygen and temperature conditions. We further predicted that temperature-dependent hypoxia tolerance varies among populations, with higher hypoxia tolerance in adults from populations experiencing more variable and/or extreme temperature and oxygen exposure (e.g. Clallam Bay, Washington, and San Diego, California, USA).

2. MATERIALS AND METHODS

2.1. Species information

Strongylocentrotus purpuratus is an invertebrate herbivorous grazer that plays a key ecological role in the function of marine ecosystems (Pearse 2006). The species has a core range along the entire west coast of North America, where it is exposed to dynamic temperature and oxygen variability in the California Current System (Ebert 2010) (Fig. 2). Recently, numbers of *S. purpuratus* have dramatically increased along the California coast, decimating kelp forests and leaving behind urchin barrens with low biodiversity and cascading ecological effects (Rogers-Bennett & Catton 2019). Like most echinoids, *S. purpuratus* undergoes a

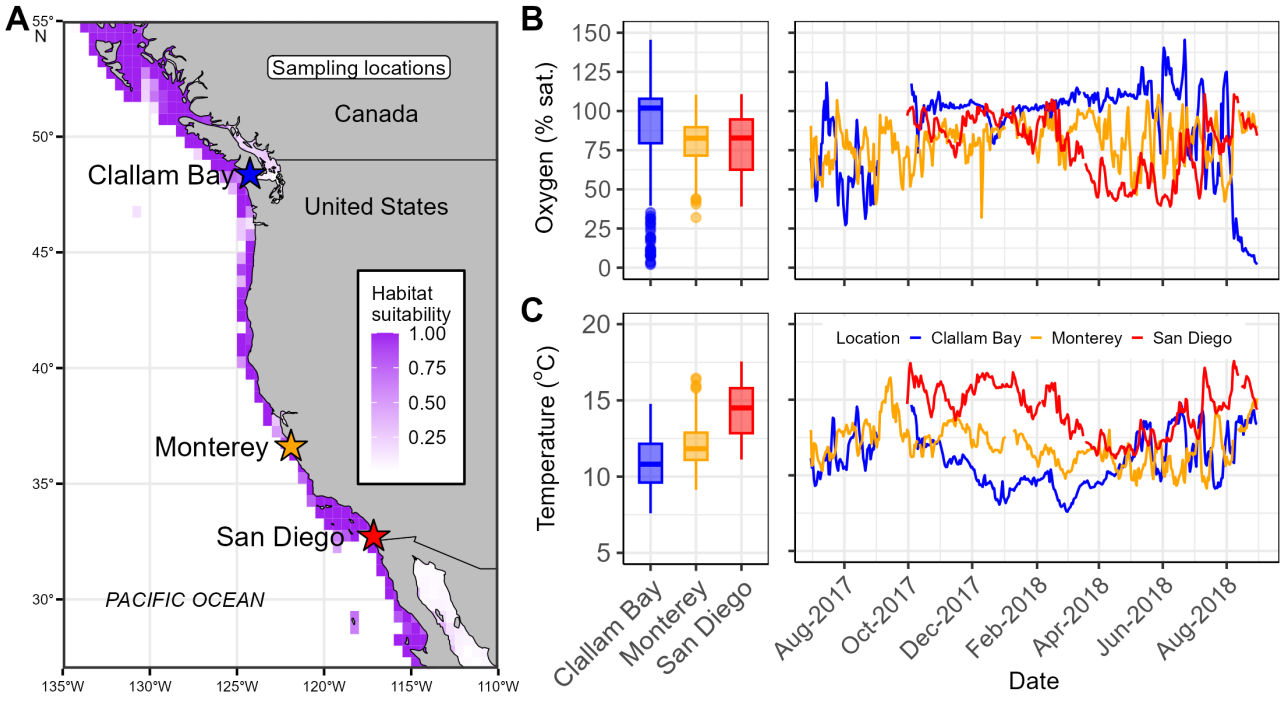

Fig. 2. Sampling locations and associated environmental conditions. (A) Geographic locations (stars) where adult *Strongylocentrotus purpuratus* specimens were collected for this study, covering a large portion of their core distribution (see Section 2 for locality information). A habitat suitability index (purple) for purple urchins obtained from AquaMaps (Kaschner et al. 2019) is also depicted. (B) Daily dissolved oxygen concentration and (C) seawater temperature during 1 yr of measurement (July 2017 – September 2018), obtained from moored instruments near the sampling locations (see Section 2 for instrument information). Box plots showing median (solid line), interquartile range (box), maximum and minimum values (whiskers) and outliers (points) of environmental data in left panel and time series in right panels indicate environmental variability for Clallam Bay, Monterey, and San Diego locations

planktonic larval period involving multiple developmental phases (Hinegardner 1969, McEdward & Miner 2001). The supply of larvae is influenced by environmental conditions which contribute to recruitment boom/busts that drive abundance patterns (Okamoto et al. 2020). *S. purpuratus* has been the focus of a rich research field in developmental (Lowe & Wray 2000), ecological (Pearse 2006), and genomic (Davidson et al. 2002, Sodergren et al. 2006) studies, with well-established protocols to spawn and rear organisms over larval to settlement phases (Strathmann 1987, Heyland & Hodin 2014, Hodin et al. 2019). For these reasons *S. purpuratus* is an ideal species for this study.

2.2. Study design

To test for temperature-dependent plasticity in hypoxia tolerance to local environmental conditions, we measured pO_{2crit} and standard metabolic rate (SMR) across temperatures that slightly exceeded those experienced in nature (5–22°C) for 3 populations of adult *S. purpuratus* distributed throughout a north–south gradient along the US west coast: (1) Clallam Bay, Washington, (2) Monterey Bay, California, and (3) San Diego, California (Fig. 2). To test for developmental variation in temperature-dependent hypoxia tolerance, we spawned and reared *S. purpuratus* in Monterey, using adult animals from Monterey Bay, and measured pO_{2crit} across temperatures (10–19°C) for 6 developmental phases, ranging from 24 h old embryos to 40 d old metamorphosized and settled urchins.

2.3. Temperature-dependent hypoxia tolerance plasticity of adult urchins

2.3.1. Sampling locations

We collected adult *S. purpuratus* from 3 locations throughout the species' core distribution in the California Current System (Fig. 2). We sampled a northern population from Clallam Bay, WA, a southern population from San Diego, CA, and combined data from a previous study on a central population from Monterey Bay, CA (Duncan et al. 2023). The north–south gradient of these sampling locations and dynamic nature

of the California Current System exposes individuals at these locations to different environmental temperature and oxygen regimes. To describe the temperature and oxygen signals at these locations, we obtained 1 yr of high-frequency oceanographic data spanning July 2017 to September 2018 from moored instruments as follows. For the San Diego site (32.813° N, 117.290° W), we obtained oceanographic data at 20 m bottom depth (PME MiniDOT) from the California Department of Fish and Wildlife. For Monterey (36.621° N, 121.899° W), we obtained oceanographic data at 17 m bottom depth (GF Signet Resistance Thermometer, In Situ RDO Pro-X) from the Monterey Bay Aquarium. For Clallam Bay, we obtained data from the nearby Coastal Endurance inshore surface mooring (Aanderaa oxygen optode 4831, Sea-Bird SBE 16plusV2 CTD) of the Ocean Observatories Initiative (47.134° N, 124.272° W) at 7 m depth (29 m bottom depth) and 6 km offshore. While the Coastal Endurance mooring is located adjacent to Clallam Bay in the open ocean, we believe it is a good proxy location because inshore marine dynamics are dominated by open ocean processes throughout the Pacific northeast (Roegner et al. 2011), and the Salish Sea, where Clallam Bay is located, predominately consists of oceanic water with high ocean exchange rates (MacCready et al. 2021). We aggregated high-frequency time-series data into daily means and converted all oxygen measurements into a common unit (% air saturation) using the 'conv_o2' function in the 'respirometry' package in R (Birk 2020).

At Clallam Bay, adult specimens were collected by hand on 11 June 2021 at low tide from submerged rockpools (shallow, ~1 m depth) at Slip Point (48.263° N, 124.255° W) and transported on ice to Friday Harbor Labs, University of Washington. Specimens were kept in a flow-through holding system where temperature matched ambient conditions until experimented upon (15–30 June 2021). In Monterey, adult specimens were obtained from the Monterey Abalone Company (36.6055° N, 121.889° W) prior to each experimental trial (17 July–20 November 2020), where they had been held in underwater cages (approximately 2 m depth) exposed to natural ocean temperatures and fed a natural kelp diet (see Duncan et al. 2023 for more details). For San Diego, adult specimens were obtained at 15 m depth near Point Loma (32.697° N, 117.256° W) by SCUBA divers from Point Loma Marine Invert Lab on 4 March and 25 April 2022 and transported overnight on ice to Stanford University, where they were held in a recirculating saltwater aquarium at 13°C until being experimented upon (10 March–31 May 2022).

2.3.2. Experimental protocol

Respirometry techniques were used to quantify SMR and critical oxygen partial pressure (pO_{2crit}) for each specimen at a specific test temperature. A single trial involved placing specimens directly into respirometry chambers (for detailed methods, following Killen et al. 2021, see Table S1 in Supplement 1 at www.int-res.com/articles/suppl/m739p129_supp1.pdf) at 12.7–13°C and subsequently adjusting the water temperature at a rate of ~1°C h^{-1} until a test temperature of 5, 7, 10, 13, 16, 19, or 22°C was reached. Temperature was then held constant (±0.4°C). Specimens were given ~24 h to adjust to novel respirometry chamber and temperature conditions and to purge any digesting food, after which intermittent flow respirometry (with 1 of 3 cycle durations, namely 5 min measure–10 min flush, 10 min measure–5 min flush, or 10 min measure–10 min flush, depending on test temperature and organism size) was run for a further ~24 h to generate the data to quantify SMR. Oxygen levels in chambers were continuously recorded with a FireSting-O_2 fiber optic oxygen meter (FSO2-4, PyroScience) connected to oxygen sensor spots (PyroScience OXSP5) positioned in a circulation loop with bare optical fibers (SPFIB-BARE, PyroScience). After ~24 h of intermittent flow respirometry, the pO_{2crit} phase of the trial began by switching off the flush pump so that oxygen could be depleted within respirometer chambers via the specimen's aerobic metabolism until no oxygen remained. The trial was then terminated. It must be noted that the closed respirometry technique to estimate pO_{2crit} results in the buildup of waste products in the chamber which lowers pH and may increase pO_{2crit} measurements, as has been demonstrated in fish species (Hancock & Place 2016, Snyder et al. 2016). Test specimens were frozen and later thawed to weigh to the nearest hundredth of a gram. We also dried specimens at 50°C for ~24 h, measured their dry mass, ashed them at 450°C for 3 h in a muffle furnace, and then measured their ashed mass to calculate a metabolic mass (dry minus ashed mass). A blank was run in an empty respirometry chamber in parallel during each trial.

2.3.3. Quantifying SMR

The mass-specific oxygen consumption rate (MO_2, mg O_2 min^{-1} g^{-1}) of each measurement period was calculated using Eq. (1) (Svendsen et al. 2016):

$$MO_2 = \left(\left(\frac{V_{re} - M}{W}\right)\left(\frac{[O_{2a}]}{t} \times 60\right)\right) - \left(\left(\frac{V_{re} - M}{W}\right)\left(\frac{[O_{2b}]}{t} \times 60\right)\left(\frac{V_{re}}{(V_{re} - M)}\right)\right) \quad (1)$$

where V_{re} is the total volume of the respirometer in ml; M is the wet mass of the specimen in g expressed as ml (assuming 1:1 g to ml water displacement); W is the mass of the specimen in g, $\frac{[O_{2a}]}{t}$ is the oxygen consumption rate during the measurement period, and $\frac{[O_{2b}]}{t}$ is the corresponding oxygen consumption rate of an empty chamber (background respiration). Oxygen consumption rates of each measurement period were calculated using the 'calc_rate' function from the 'respR' package in R (Harianto et al. 2019). Erroneous oxygen consumption rate measurements were filtered out using an $R^2 > 0.95$ quality threshold and removing measurements associated with background respiration rates outside the 95th and 5th quantiles of all measurements, which may have occurred during temperature adjustments in the respirometry system. SMR was estimated as the 0.1 quantile of all remaining oxygen consumption measurements (Claireaux & Chabot 2016).

2.3.4. Quantifying pO_{2crit}

The oxygen drawdown curve from the pO_{2crit} phase of the experiment was split into 5 min segments with mass-specific oxygen consumption rates calculated for each segment as per the SMR protocol. All MO_2 measurement segments were paired with the corresponding average oxygen concentration values converted to percent saturation using the 'conv_o2' function in the 'respirometry' package (Birk 2020). We defined pO_{2crit} for adults as the lowest level of oxygen at which an animal can maintain SMR (Ultsch & Regan 2019). We estimated this level following the protocol of Seibel et al. (2021) using the 'calc_pcrit' function in the 'respirometry' package, where pO_{2crit} is taken as SMR divided by oxygen supply capacity (α_s) — the highest value of metabolic rate measurements divided by corresponding oxygen partial pressure $\left(\frac{MO_2}{pO_2}\right)$ for all measurement segments of the oxygen drawdown curve. This α-method showed congruence with estimates of pO_{2crit} using the limiting low oxygen method described by Claireaux & Chabot 2016) (Fig. S1) and ensured comparability with larval pO_{2crit} estimates where SMR was not explicitly quantified.

2.3.5. Analysis

For SMR, we first estimated the allometric scaling exponent for mass (δ). We removed the effect of temperature from the data by dividing with the Arrhenius-Boltzmann function following Deutsch et al. (2015). We estimated δ as the slope of the linear relationship between the natural logarithms of temperature-standardized SMR and body mass (B) (Brown et al. 2004). We then mass-standardized SMR data by multiplying each SMR measurement by the ratio of the corresponding test specimen's body mass (B) and its mass raised to the power of the allometric scaling exponent $\left(\frac{B}{B^{\delta}}\right)$. We modeled the effect of temperature on mass-standardized SMR for each sampling location with an Arrhenius model described in Eq. (2) (Gillooly et al. 2001):

$$SMR = \alpha_d . e^{E/kT} \quad (2)$$

where α_d is the rate coefficient, E is activation energy, k is Boltzmann's constant (eV), and T is absolute temperature in Kelvin.

We estimated the constants of the Arrhenius models for each sampling location, α_d and E, as the back-transformed intercept and slope of the linear relationship between the natural logarithm of mass-standardized SMR and the inverse of kT (product of Boltzmann constant k and temperature T in Kelvin), respectively. To test for significant differences in the parameters of Arrhenius models among sampling locations, we combined all data, fit linear models to the relationship between mass-standardized SMR and temperature, and included 'site' as a full interaction term in the linear models using Clallam Bay or San Diego as the reference population.

pO_{2crit} may be higher than predicted by an Arrhenius model at colder temperatures (Boag et al. 2018, Duncan et al. 2020, Endress et al. 2024). We therefore fit more flexible quadratic polynomial models through the relationship between pO_{2crit} and temperature following Eq. (3):

$$pO_{2crit} = a.t + b.t^2 + c \quad (3)$$

where t is temperature in Celsius, and a, b, c are model parameters. To test for a significant difference in the relationship between temperature and pO_{2crit} among sampling locations, we also included 'site' as a full interaction term in quadratic polynomial models with Clallam Bay or San Diego as reference populations. For both SMR and pO_{2crit} analyses, we shifted temperature data such that the intercept corresponded to the lowest temperature tested.

2.4. Temperature-dependent hypoxia tolerance over developmental stages

The development of *Strongylocentrotus purpuratus* over embryonic, larval, metamorphosis, and settlement stages was reviewed in detail by Pearse & Cameron (1991). Briefly, following fertilization, the zygote undergoes multiple cleavage transitions until a hollow sphere of cells called a blastula hatches (~24 h post fertilization [hpf]). Gastrulation then occurs where the invagination and elongation of a vegetal plate forms a rudimentary alimentary cavity (~48 hpf). Embryos then differentiate into a larval structure via a prism phase (~72 hpf) and subsequently into an early-pluteus phase where feeding begins, and juvenile structures develop in the rudiment. However, this rate of development is extremely temperature sensitive and can vary multiple fold among temperature exposures. After 1–3 mo in the planktonic pluteus phase, larvae metamorphose and settle onto the substrate where their morphology is similar to a juvenile urchin.

2.4.1. Larval rearing

We spawned and reared multiple batches of *S. purpuratus* larvae from fertilized embryos to settlement stage at Hopkins Marine Station, Monterey, from 1 March – 4 May 2021 following the protocol outlined by Hodin et al. (2019). Ripe adults were obtained from the Monterey Abalone Company on 4 December 2020, kept in the dark in flow-through aquaria, and fed an abundance of kelp to maintain gonadal condition. To induce the release of gametes, ripe urchins were injected with roughly 1–3 ml of 0.5M potassium chloride through the peristomial membrane around their mouths. Eggs were harvested in sterilized seawater beakers and a few drops of 1% diluted sperm were added to induce fertilization. Fertilized eggs were kept in 1 l beakers placed in a flow-through seawater table to maintain ambient ocean temperature in the beaker (~13°C) at a low density where they developed through blastula (24 hpf), gastrula (48 hpf), and prism (72 hpf) phases. After 96 hpf, larvae were transferred into 20 l plastic containers, filled with sterilized seawater, placed in a flow-through sea table to maintain ambient ocean temperature, and aerated through the bottom to create a gentle flow and keep larvae in suspension. Densities were kept low (<1 ind. ml^{-1} at first) to ensure uniform size distributions and consistent stages of development. Once the early-pluteus phase was reached, concentrated (between ~2 and 5 million cells ml^{-1}) microalgae (*Rhodomonas lens*) were added ad libitum into the rearing container as a food source. Every 2–3 d, the water was changed, and fresh microalgae were added. We continued this process for 33 d until the late-pluteus phase. To stimulate metamorphosis and induce settlement, we added pebbles from the Monterey Bay rocky shore into the container with the larvae. Post settlement, we slowed down the frequency of water changes as new recruits fed on turf algal growth inside the rearing vessels. Culture temperatures were maintained at ambient seawater temperatures throughout, which fluctuated around 13°C.

2.4.2. Experimental protocol

We measured larval respiration rates using 2 SDR 24-channel SensorDish (PreSens Precision Sensing) instruments connected in parallel with 24-well glass microplates (80 µl volume, Loligo Systems). Each microplate was placed inside a water bath on top of the SDR reader where fresh water was continuously circulated through a high precision water bath to manipulate and maintain temperatures. We measured respiration rates at 6 developmental stages; blastula (24 hpf), gastrula (48 hpf), prism (72 hpf), early-pluteus (8 d post fertilization [dpf]), late-pluteus (28/29 dpf), and settlement phases (36/37 dpf) at 4 temperatures that span the natural range experienced by larvae in the California Current System: 10, 13, 16, and 19°C. For each temperature, user-defined calibrations were set by taking average phase values of wells filled with 100% air-saturated seawater and 0% air-saturated seawater created with sodium sulfite. For each trial, a batch of larvae were obtained from the culture by draining rearing vessels through an appropriately sized dry collection sieve and placing larvae into a glass beaker filled with sterilized seawater floated in a water bath at 13°C (same as rearing temperature). The temperature of the water bath was then adjusted at ~1°C h^{-1} until the test temperature was reached. Larvae were given 2 h to acclimate, which was constrained by the time needed to reach pO_{2crit} before new development stages occurred. Larvae were then added into the microplate wells, at various concentrations depending on supply to assess density effects on pO_{2crit} (ranging from a minimum of 640 to a maximum of 10 120 individuals per well for blastula, 2040–7600 for gastrula, 1120–5000 for prism, 400–1960 for 4-arm pluteus, 2–72 for 8-arm pluteus, and 3–10 for settled developmental stages; see Supplement 2 at www.int-res.com/articles/suppl/m739p129_supp2.xlsx for more details), with a transfer pipette so that the meniscus was seen above the well level. At least 6 wells were

filled with 100% air-saturated seawater only as a blank to ensure that no background respiration was present. The microplate wells were sealed with parafilm and covered with a silicon pad and compression block, such that no temperature-controlled freshwater mixed into wells, and covered with aluminum foil so no light entered the respirometry system. Oxygen levels were recorded in each well with supplied SDR reader software and logged to an excel sheet every 15 s. Oxygen in the chamber was drawn down by larvae until none remained, upon which the trial was terminated. Each trial consisted of multiple wells measured at a single temperature for a developmental phase such that replicates in subsequent analyses were the wells per developmental phase/temperature (see Supplement 2 for details). We spawned and reared 2 batches of larvae sequentially, each from several male and female gametes mixed together and did not track parental/genotype effects further. Following each trial, larvae were transferred to test tubes, relaxed in 3.5% $MgCl_2$ seawater solution for 10 min, and then fixed in 4% formaldehyde in seawater solution. Larvae were counted several months later and photographed to accurately record the stages. Later, test tubes filled with fixed larvae were centrifuged, and the fix solution was pipetted out and replaced with 1000 µl of phosphate-buffered solution. Test tubes were then shaken to evenly suspend larvae, and total numbers of larvae per well were estimated by counting the number of larvae in 5 pipette drops (5 µl volume each), taking the average and back-calculating for early developmental stages. The total number of larvae for late stages (8-arm and settled individuals) were entirely counted. Larvae were photographed under magnification using a Leica DMi1 inverted microscope for cell culture.

2.4.3. Quantifying pO_{2crit}

Respiration rates per individual can suffer from density-dependent inhibition when larval concentrations exceed a certain threshold (Marsh & Manahan 1999). We did not standardize for density but recorded it per well to make sure variability in density did not influence pO_{2crit} data. For this reason, we do not report an SMR per individual larva. We use the α-method to estimate pO_{2crit} for larval wells but benchmark it against an average oxygen consumption rate of each well, assuming that individual pO_{2crit} would occur around an average pO_{2crit} per well and that temperature has a more pervasive effect on metabolic rates than well density. We considered a measurement successful if oxygen levels decreased in a linear trend and leveled off below 5% and above 0% saturation. For each drawdown curve, we excluded data above an oxygen level of 70% saturation, as oxygen readings needed time to adjust following addition of larvae. The remaining drawdown curves from each well were split into 100 time intervals, and oxygen consumption rate per well (RO_2) was estimated using the 'calc_MO2' function in the respirometry package (Birk 2020) and paired with corresponding mean oxygen level (% saturation). We used all oxygen consumption rate measurements between 40 and 70% saturation to calculate the average oxygen consumption per well. We chose this threshold as it was between the time when oxygen levels in blanks stabilized and before oxygen levels began limiting metabolic rates. For each well, we estimated oxygen supply capacity (α_s) as the highest value of $\alpha\left(\frac{RO_2}{pO_2}\right)$. To estimate pO_{2crit}, we divided the average oxygen consumption in each well by its corresponding α_s value. We explored density effects on pO_{2crit} by fitting linear models to the relationship between pO_{2crit} and well density for each developmental stage and the temperature tested.

2.4.4. Analysis

For each stage of development (blastula, gastrula, prism, early-pluteus, late-pluteus, settlement, and Monterey adults), we modeled pO_{2crit} as a function of temperature using an Arrhenius model (same as Eq. 2 but with pO_{2crit} as the response variable). For each developmental stage, we estimated the Arrhenius model coefficient (α_d) as the back-transformed intercept and temperature sensitivity (E) as the slope from the linear relationship between the natural logarithm of pO_{2crit} and the inverse of kT (product of Boltzmann constant k and temperature T in Kelvin). We qualitatively compared developmental changes in temperature sensitivity (E) and overall hypoxia tolerance (pO_{2crit}), taken as the predicted pO_{2crit} at 14.5°C (midpoint temperature of the experiment), from developmental stage-specific Arrhenius models.

3. RESULTS

3.1. Temperature-dependent hypoxia tolerance plasticity of adult urchins

3.1.1. Environmental conditions

Our 3 sampling locations are exposed to different temperature and oxygen regimes in the California

Current System (Fig. 2). Temperature decreased from southern (San Diego) to northern (Clallam Bay) locations, but temperature variability was similar. San Diego had a mean temperature of 14.3°C, ranging between 11.1 and 17.6°C, Monterey had a mean temperature of 12.0°C (9.1—16.5°C), and Clallam Bay had a mean temperature of 10.9°C (7.6—14.8°C). Oxygen availability was generally above 70% air saturation at all locations. However, patterns varied seasonally among the 3 locations. Mean oxygen concentration at San Diego was 78.2% air saturation, ranging between 39 and 110.7%, Monterey had a mean of 90.1% air saturation (32 — 110.4%), and Clallam Bay had a mean of 90.2% air saturation (2—145.5%). During the upwelling season, April to June, oxygen saturation remained high at Clallam Bay, intermediate and variable in Monterey, and lower, around or below 50% saturation, in San Diego. Oxygen saturation was high in late summer in Monterey and San Diego, but was more variable at Clallam Bay. At this location, oxygen became at times hyperoxic, but also suddenly dropped to values near anoxia, likely driven by photosynthesis and inshore upwelling variability, respectively (Roegner et al. 2011). While a quantitative analysis is beyond the scope of this study, these patterns are consistent with the oceanographic literature for these areas (Roegner et al. 2011, Jacox et al. 2019, Howard et al. 2020a, Low et al. 2021, Renault et al. 2021). We therefore consider the sampling location temperatures to range from warm (San Diego) to cold (Clallam Bay) in terms of temperature and consider oxygen availability to be similar at all locations on average, but seasonally variable, with Clallam Bay experiencing severe intermittent hypoxic events.

3.1.2. SMR

Overall, we quantified SMR for 170 adult urchins (n = 97 for Monterey, n = 39 for Clallam Bay, n = 34 for San Diego). Sample number across temperature treatment and sampling location ranged from 2 (San Diego, 5°C) to 22 (Monterey, 16°C) and is shown in full in Table S2. SMR is well approximated by Arrhenius models (Fig. 3) and varies significantly between Clallam Bay (reference population in Table 1) with Monterey and between Monterey and San Diego (reference population in Table S3). We found a significant difference in SMR—temperature relationships between Clallam Bay and Monterey (Table 1), a weakly significant difference between Clallam Bay and San Diego (Table 1), and no significant difference between San Diego and Monterey (Table S3). Overall, the Clallam Bay population was

Table 1. Modeling results of natural logarithm of standard metabolic rate as a linear function of Arrhenius temperature with sampling location as full interaction term (Clallam Bay is the reference population). R^2 = 0.8871, df = 5, 164, F = 257.6. Significant p-values (p < 0.05) are highlighted in **bold**

Effect	Estimate	SE	*t*	p
Intercept	−0.827	0.058	−14.169	**<0.0001**
Monterey	0.398	0.072	5.498	**<0.0001**
San Diego	−0.045	0.094	−0.479	0.633
Arrhenius temp	−0.841	0.042	−20.053	**<0.0001**
Arrhenius temp: Monterey	0.211	0.052	4.064	**<0.0001**
Arrhenius temp: San Diego	0.166	0.066	2.512	**0.013**

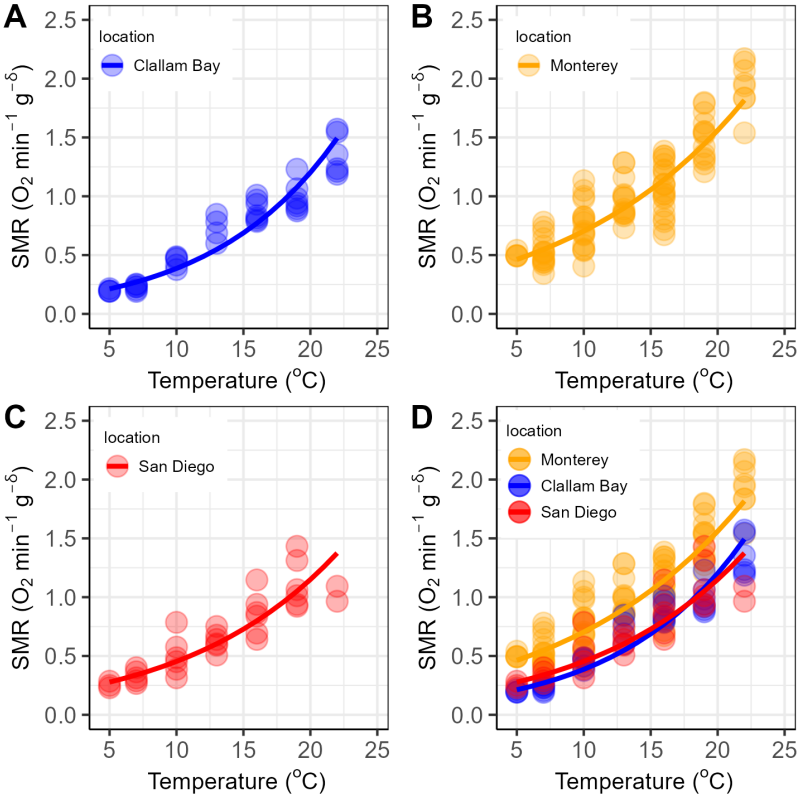

Fig. 3. Standard metabolic rates (SMRs) of adult purple sea urchins. SMR data (points) fit with Arrhenius models (solid lines) for each sampling location: (A) Clallam Bay, (B) Monterey, (C) San Diego, and (D) all locations combined

more sensitive to warming temperatures, although the data from this site had the worst fit with the Arrhenius model (Table 1; Table S4 for Arrhenius model parameters). Across all temperatures, between 5 and 22°C, the Monterey population had the highest SMRs (Fig. 2; Fig. S2).

3.1.3. pO_{2crit}

Overall, we quantified pO_{2crit} for 164 adult urchins (n = 91 for Monterey, n = 39 for Clallam Bay, n = 34 for San Diego). Sample number across temperature treatment and sampling location ranged from 2 (San Diego, 22°C) to 21 (Monterey, 16°C) and is shown in full in Table S5. Overall hypoxia tolerance (pO_{2crit}) of adult urchins was not significantly different among sampling locations, despite the different environmental regimes they were exposed to (Table 2; Table S6). The relationship between pO_{2crit} and temperature was well approximated by a quadratic polynomial for all 3 sampling locations (Fig. 4; see Table S7 for model parameters). We did detect some weakly significant temperature shape parameters between Clallam Bay and Monterey and San Diego (Table 2). Temperature had a limited effect on pO_{2crit} between 5 and 13°C, after which pO_{2crit} increased substantially, indicating less hypoxia tolerance at warmer temperatures.

3.2. Temperature-dependent hypoxia tolerance over developmental stages

Overall, we quantified pO_{2crit} for 110 wells (out of 194 attempts) of larvae from the Monterey population. The other 84 (43%) wells failed to reach a reliable pO_{2crit} either because respiration rates were so low that time to consume all oxygen exceeded the time taken to reach the next developmental stage, oxygen levels in wells leveled off above the 5% saturation threshold (indicating a calibration issue), or oxygen levels increased (indicating a leak). Replication per temperature–stage treatments ranged from 1 well (10°C) to 4 wells (16°C) for blastula, 2 (19°C) to 9 (16°C) for gastrula, 5 (16°C) to 13 (13°C) for prism, 4 (10, 13, 16°C) to 9 (19°C) for 4-arm pluteus, 2 (10°C) to 5 (16°C) for 8-arm pluteus, and 2 (10, 16°C) to 4 (13, 19°C) for settled stages (see Table S8 for more details). pO_{2crit} data were well approximated by Arrhenius models for all stages of development between 10 and 19°C (Fig. 5; Table S9 for Arrhenius model parameters), with pO_{2crit} increasing with temperature for every developmental stage. From blastula to set-

Table 2. Modeling results of critical oxygen level as a quadratic function of temperature with sampling location as full interaction term (Clallam Bay is the reference population). R^2 = 0.692, df = 8, 155, F = 43.44. Significant p-values (p < 0.05) are highlighted in **bold**

Effect	Estimate	SE	t	p
Intercept	11.014	1.637	6.728	**<0.0001**
Temp	−1.386	0.460	−3.016	**0.003**
Temp^2	0.153	0.259	5.877	**<0.0001**
San Diego	−3.596	2.480	−1.450	0.149
Monterey	0.155	2.040	0.076	0.939
Temp: San Diego	1.426	0.697	2.045	**0.043**
Temp: Monterey	1.383	0.564	2.451	0.057
Temp^2: San Diego	−0.078	0.041	−1.915	0.058
Temp^2: Monterey	−0.094	0.032	−2.953	**0.003**

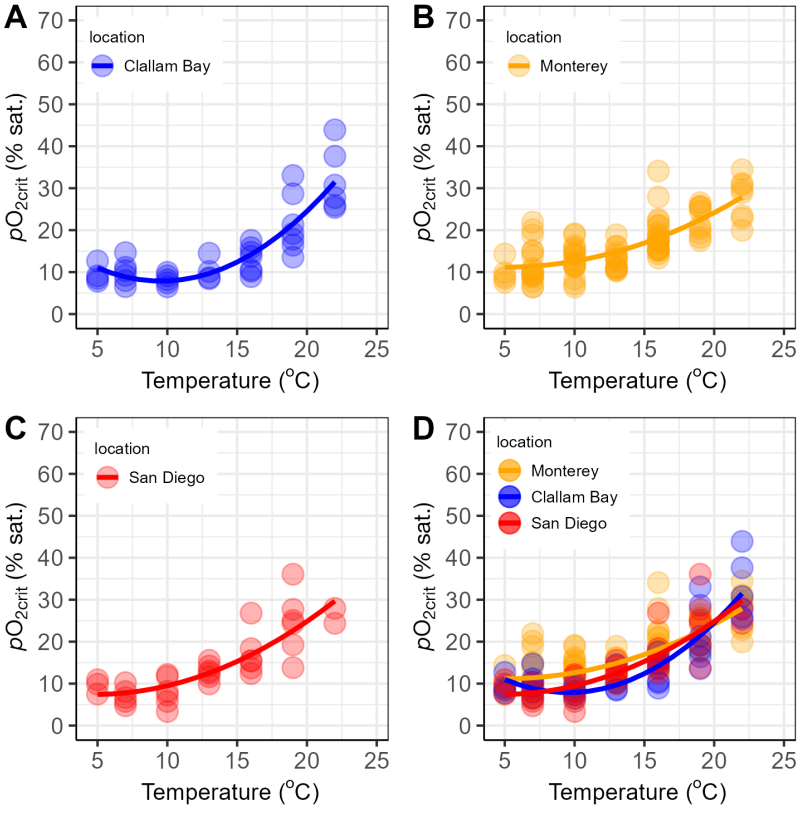

Fig. 4. Temperature-dependent hypoxia tolerance of adult purple sea urchins. Critical oxygen partial pressure (pO_{2crit}, % air saturation) data (points) fit with quadratic polynomial models (solid lines) for each sampling location: (A) Clallam, (B) Monterey, (C) San Diego, and (D) all locations combined

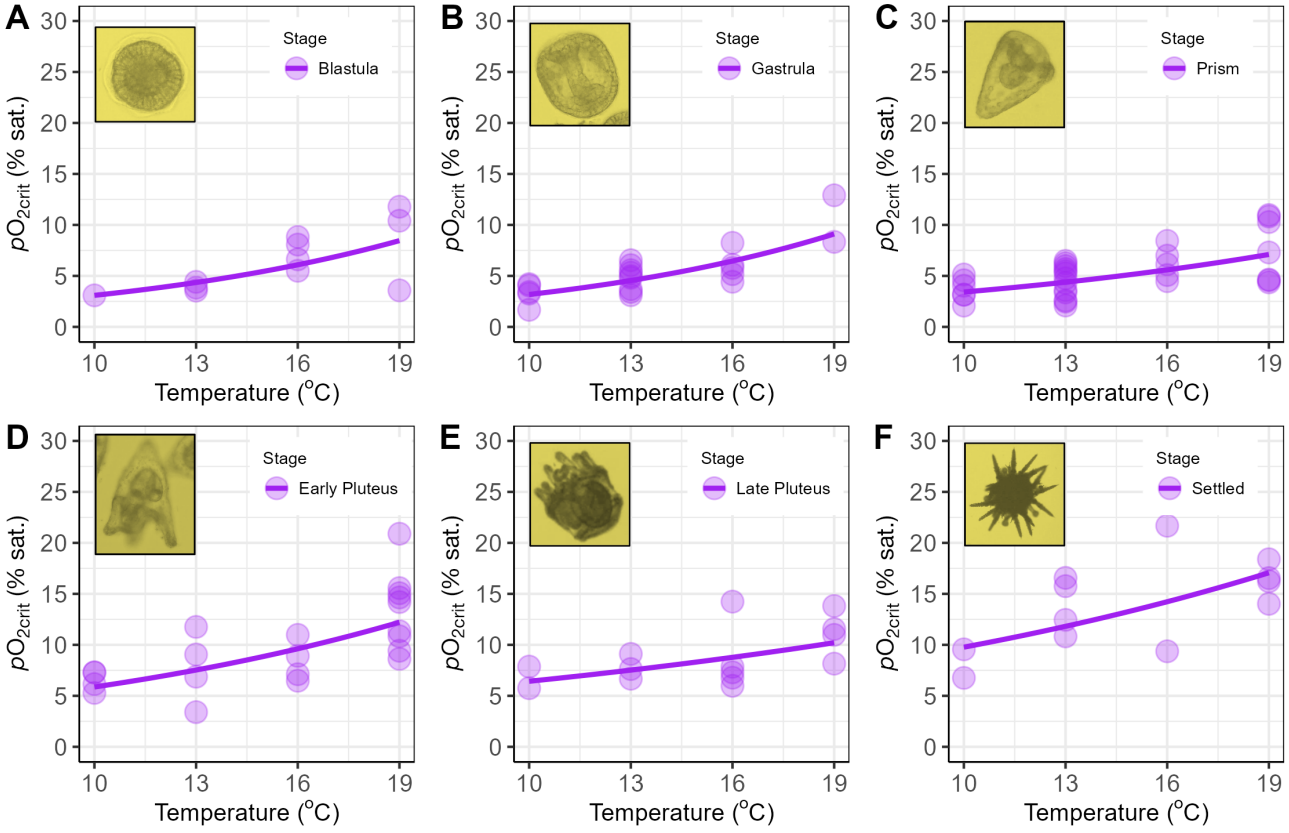

Fig. 5. Temperature-dependent hypoxia tolerance of larval purple sea urchins. Critical oxygen partial pressure (pO_{2crit}, % air saturation) data (points) fit with Arrhenius models (solid lines) for each stage of larval development: (A) blastula, (B) gastrula, (C) prism, (D) early-pluteus, (E) late-pluteus, and (F) settled. Images are not to scale

tlement and for temperatures from 10 to 19°C, pO_{2crit} remained below 20% air saturation, indicating high temperature-dependent hypoxia tolerance compared with adults. Parameters of Arrhenius models showed clear patterns with ontogenetic development (Fig. 6). Temperature sensitivity (E) decreased with development stage until larvae settled (Fig. 6B). In contrast,

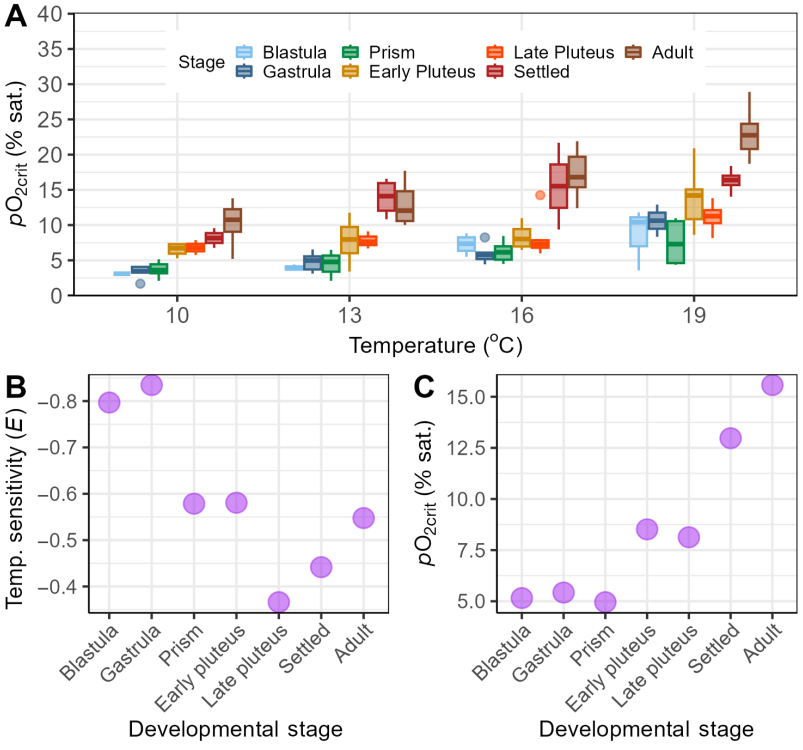

Fig. 6. Hypoxia tolerance over development in purple sea urchins. (A) Comparative hypoxia tolerance (critical oxygen partial pressure, pO_{2crit}, % air saturation) for each larval development stage and adults from Monterey by temperature. Box plot description as in Fig. 2. Temperature-dependent hypoxia tolerance traits from Arrhenius models for each stage of larval development and adults from Monterey: (B) temperature sensitivity (E) across temperature range, and (C) Arrhenius model critical oxygen partial pressure (pO_{2crit}, % air saturation) predictions at the midpoint temperature of 14.5°C

hypoxia tolerance (pO_{2crit} at 14.5°C) was greater (low pO_{2crit}) for embryonic stages (blastula–prism) and decreased (pO_{2crit} increased) throughout larval to adult phases (Fig. 6A). Thus, early larval stages of *S. purpuratus* were most sensitive to temperature variability, but least sensitive to low oxygen levels, while adults were least sensitive to temperature, but most sensitive to hypoxia (Fig. 6B,C). We also found little influence of well density on pO_{2crit}, with only 1 weakly significant linear relationship (gastrula at 13°C) among 24 tested for each larval stage/temperature with 9 positive, 10 negative, and 4 unquantifiable slope parameters (Table S10, Figs. S3–S6), as would be expected by random chance. We did observe pervasive effects of temperature on per individual metabolic rates for each larval stage, which produced a greater effect than within metabolic rate variability at each temperature (Fig. S7).

4. DISCUSSION

The relatively low pO_{2crit} values of *Strongylocentrotus purpuratus*, compared with other marine species (e.g. Fig. S5A in Penn et al. 2018), for all developmental phases and temperatures tested and from all sampling locations, indicate a generally high hypoxia tolerance across temperature. This is in accordance with previous research on *S. purpuratus*, where adults were reported to survive up to 60 h in water with minimal oxygen levels (~10% air saturation) (Low & Micheli 2018) and where larval mortality in near anoxic water (<10% air saturation) was no different than that in fully aerated water (Eerkes-Medrano et al. 2013). While mass mortality events of *S. purpuratus* in California have occurred and been attributed to low salinity (Hendler 2013) or harmful algal blooms (Jurgens et al. 2015), our results suggest it is unlikely that deoxygenation will exceed the species' tolerance threshold across the range of temperatures regularly experienced in the wild, although the species will be vulnerable to deoxygenation during severe marine heatwaves. Compromised performance for *S. purpuratus,* however, can occur at oxygen levels higher than the pO_{2crit} if additional processes (e.g. digestion, movement, feeding, growth, calcification) become oxygen limited (Low & Micheli 2020, Ng & Micheli 2020) and lethal effects of warm temperature can manifest in fully saturated water before crossing a species' hypoxia threshold (Ern et al. 2017). *S. purpuratus* does, however, have the ability to suppress its metabolic demand when conditions are suboptimal for extended periods of time and re-establish normal functioning when better conditions return (Dolinar & Edwards 2021). In the context of ocean warming and deoxygenation in the California Current System, and based off our temperature-dependent hypoxic thresholds for aerobic metabolism, we posit that *S. purpuratus* can be considered resilient to deoxygenation.

4.1. Temperature-dependent hypoxia tolerance across adult urchin populations

We observed similar temperature-dependent hypoxia tolerance relationships for all 3 populations of *S. purpuratus* despite the different thermal and oxygen regimes they are exposed to in their source locations. These results indicate that *S. purpuratus* may have limited plasticity for this trait or for plasticity-related physiological functioning, ensuring that optimal pO_{2crit}–temperature relationships are maintained. Whether thermal acclimation can alter hypoxia tolerance of aquatic species is not clear, due to a paucity of appropriately designed studies (Collins et al. 2021). For those studies where pO_{2crit} at any metabolic level is measured in organisms acclimated to various temperature periods, evidence is limited and varied. For example, pO_{2crit} at 25°C for the triplefin fish *Bellapiscis lesleyae* was significantly improved following acclimation to temperatures of 20 vs. 15°C, while it did not change in the related species *B. medius* (Hilton et al. 2008). No beneficial effect of temperature exposure duration on pO_{2crit} was reported for black sea bass *Centropristis striata* (Slesinger et al. 2019) or Doederlein's cardinalfish *Ostorhinchus doederleini* and lemon damselfish *Pomacentrus moluccensis* (Nilsson et al. 2010). Studies testing for thermal acclimation effects on hypoxia tolerance using the time to loss of equilibrium (LOE) metric have reported a positive effect of acclimation to warmer temperatures in brook charr *Salvelinus fontinalis* (Jensen & Benfey 2022) and Atlantic killifish *Fundulus heteroclitus* (McBryan et al. 2016).

We found no difference in temperature-dependent hypoxia tolerance among sampling locations, despite significantly higher resting oxygen demand (SMR) for the Monterey population compared to both San Diego and Clallam Bay across all temperatures tested. The elevated resting metabolism for Monterey was unexpected considering exposure to less extreme temperatures compared to the other 2 sites. The most likely explanation is that the elevated SMR of the Monterey population is due to sample specimens

being obtained from an *in situ* aquaculture operation where they were fed ad libitum (Nilsson-Örtman & Brönmark 2022). Variable oxygen demands yet similar hypoxia tolerances among populations indicate that oxygen supply capacity is plastic, resulting in consistently optimal pO_{2crit}, perhaps to maintain levels of aerobic scope (Seibel & Deutsch 2020, Seibel et al. 2021).

4.2. Temperature-dependent hypoxia tolerance over developmental stages

We found high hypoxia tolerance (pO_{2crit} < 15% air saturation) for all embryonic and larval development phases (blastula to settlement) of *S. purpuratus*. There is limited information for marine larvae pO_{2crit}, most likely because of the challenges associated with measuring metabolic rates for such tiny specimens (Peck & Moyano 2016). However, those studies that have measured larval hypoxia tolerance report relatively high pO_{2crit} (low hypoxia tolerance). For example, pO_{2crit} for pre-settlement larvae of black-axil chromis *Chromis atripectoralis* and Ambon damsel *Pomacentrus amboinensis* are estimated at 45 and 43% air saturation, respectively (Nilsson et al. 2007), while pre-settlement Dover sole *Solea solea* larvae have a pO_{2crit} reported at 12.6 kPa (~50% air saturation) (McKenzie et al. 2008). The only study investigating temperature-dependance of hypoxia tolerance at various larval stages of an invertebrate species, the Atlantic rock crab *Cancer irroratus*, reported relatively high lethal oxygen limits and temperature sensitivities corresponding to hypoxic thresholds close to 100% air saturation in warm water (30°C) (Vargo & Sastry 1977). Such findings have contributed to the proposition that early life stages of development are generally less tolerant to hypoxia (Vaquer-Sunyer & Duarte 2008; see review by Eerkes-Medrano et al. 2013). However, these studies either worked on larval fish where bone development phases can be especially energetically expensive and do not explicitly quantify metabolic demand (Edworthy et al. 2018), or used metrics based on larval survival, which can be hard to disentangle from hypoxia-induced mortality as larval mortality is naturally high. A comparable recent study to ours quantifying pO_{2crit} of the Australian hybrid abalone found values ranging from 22.7% air saturation in fertilized eggs to 14% in mid-veliger larvae (Alter et al. 2016), which are slightly higher but in line with our study. Our results are also in accordance with the only previous study on *S. purpuratus* larval hypoxia tolerance, where Eerkes-Medrano et al. (2013) reported no difference in survival of pluteus larvae from Oregon when exposed to 'near anoxia' (<0.5 ml l^{-1}, ~7.4% saturation at temperature of ~9°C) vs. control (5–7 ml l^{-1}, ~74–104% saturation at temperature of ~9°C) water. These results are consistent with theoretical considerations that larvae should have lower hypoxic thresholds than adults (Sperling et al. 2015). Whether this finding for *S. purpuratus* applies to more direct developers like fish needs to be tested further.

The observed high hypoxia tolerance suggests it is unlikely that deoxygenation events will be a proximate cause for *S. purpuratus* larval death at temperatures between 10 and 19°C while in the plankton of the California Current System. Juvenile *S. purpuratus* recruitment is variable in space and time throughout the California Current, with recruitment anomalies driving population booms (Rogers-Bennett 2013, Rogers-Bennett & Okamoto 2020). These recruitment pulses are driven by larval supply, which varies with ocean temperature and El Niño–Southern Oscillation-driven current patterns across California (Okamoto et al. 2020). Indeed, temperature is a fundamental driver of invertebrate larval development (Hoegh-Guldberg & Pearse 1995) and specifically for *S. purpuratus* (Azad et al. 2012), but our results indicate it is unlikely to interact with oxygen in an energetically limiting way for this species. However, we only quantified the absolute minimum oxygen level required to maintain levels of aerobic metabolism, and it is possible that exposure to deoxygenation levels above this pO_{2crit} threshold during early embryonic phases may hinder development and contribute to recruitment failure. For example, Layous et al. (2021) found that early hypoxia exposure in a closely related sea urchin (*Paracentrotus lividus*) can impede gene regulatory networks, impairing skeletal and growth development, although the deoxygenation treatments in that study were close to anoxia and notably below our measured pO_{2crit} of *S. purpuratus.*

We identified distinct patterns in temperature-dependent hypoxia tolerance throughout ontogenetic development phases (Fig. 6) that can be explained by developmental morphology and function. Temperature sensitivity (E) decreased with development from blastula to late-pluteus, while overall hypoxia tolerance remained consistent during embryonic phases (blastula to prism), but decreased (higher pO_{2crit}) following the transition to early-pluteus (Fig. 6A,B). Oxygen is supplied to the developing animal embryos via diffusion across the egg surface area,

while the rate of internal energy conversion fueling growth and differentiation sets oxygen demands (Pearse & Cameron 1991, Martin et al. 2020). If total metabolic oxygen demand increases with egg volume, then supply via surface area diffusion will fail to meet this demand at increasingly higher oxygen levels, resulting in a higher pO_{2crit} (Martin et al. 2020). The consistently low pO_{2crit} measured across embryonic stages (blastula to prism) suggests that either metabolic oxygen demand does not increase, despite an increase in volume, or that oxygen supply increases through changes in membrane permeability with development. This was confirmed by Meyer et al. (2007), who reported no difference in individual metabolic rates for *S. purpuratus* embryos over the first 4 d of development. We did, however, find a ~2-fold increase in temperature sensitivity (*E*) for these embryonic phases compared to later phases. Warming increases rates of biochemical reactions and hence oxygen demand following an exponential relationship (Gillooly et al. 2001), while supply remains relatively constrained by a lower rate of oxygen diffusivity increases (Han & Bartels 1996) and by diffusion over a fixed surface area, causing pO_{2crit} to be reached at increasingly higher oxygen levels with warming (Martin et al. 2020). Following the transition from prism to early-pluteus, overall hypoxia tolerance progressively decreases, which coincides with the onset of larval feeding, active swimming, skeletal development (Smith et al. 2008), and the subsequent increase in per individual metabolic oxygen demand (Meyer et al. 2007). However, the onset of feeding may contribute to the simultaneous reduction in temperature sensitivity (*E*). To feed and swim, pluteus larvae pass water along their arms via ciliated beats into their mouth, which drives water exchange, replenishing an oxygen diffusion gradient and maintaining respiration rates (Strathmann 1971). If warming speeds up ciliated beat frequency and swimming speeds, the subsequent increase in metabolic oxygen demand may be accompanied by greater rates of oxygen supply, dampening the temperature effect that would otherwise drive pO_{2crit} higher.

There are several caveats with the experimental design in this study that caution against drawing generalizable conclusions and extrapolating beyond the species and system investigated here. First, the study involved 21 temperature–location treatment combinations for the adult study and 24 temperature–developmental stage treatment combinations for the larval study, which resulted in some treatments not being replicated sufficiently (i.e. no replication for blastula at 10°C). While we fit regression models across the range of temperatures for each developmental stage and/or sampling location, when replication levels are low at the lowest/highest temperatures, it is possible for anomalous measurements to have a disproportionate effect on regression model parameters. Furthermore, there are several confounding variables that were not explicitly considered but may have influenced the results of the study. Adult specimens were collected from different habitats, namely in the ocean at depths around 15 m in San Diego, from a nearshore ocean-based aquaculture facility in Monterey, and from an intertidal environment in Clallam Bay. Given commonly fluctuating temperatures in intertidal environments, it is possible that the Clallam Bay organisms may have (at times) experienced warmer conditions than the subtidal San Diego specimens despite being from the more northern locality (i.e. depth and geography are confounding variables). Nonetheless, at a broad level, we have clearly sampled 3 unique populations of *S. purpuratus* for physiological comparison. The acclimation protocol prior to experimentation was also different with recirculating tanks for San Diego, ocean cages for Monterey, and flow-through systems for Clallam Bay. These confounding exposures may have influenced measurements (i.e. higher SMRs for the Monterey population from an aquaculture farm). The fact that hypoxia tolerance is similar despite different levels of baseline respiration recorded here suggests that our findings of consistent adult hypoxia tolerance among populations is robust. Similarly, with the larval study, acute thermal shock (2 h) and variable densities among wells may have influenced respiration rates, but the consistent patterns between hypoxia tolerance and development for each temperature tested indicates a level of robustness to the patterns observed. Nevertheless, it is important that more studies test hypoxia tolerance across a wide range of temperatures and multiple populations before any generalizations can be made.

Overall, the interaction of developmental phase-specific pO_{2crit} Arrhenius model parameters (Table S9) results in hypoxia tolerance of adults being lower (higher pO_{2crit}) than any earlier developmental stage at any temperature currently experienced throughout the core distribution of *S. purpuratus* in the California Current System. This was unexpected, as larvae are generally considered more sensitive to environmental extremes than adults. The consistency of temperature-dependent hypoxia tolerance among adult populations, despite exposure to different thermal and oxygen regimes, suggests this critical threshold may not be able to

change or that related physiological process are plastic such that pO_{2crit} remains optimally low. These findings agree with another study that quantified pO_{2crit} for an aquatic organism (barramundi *Lates calcarifer*) at multiple locations and temperatures (Collins et al. 2013). Because oxygen demand varied among populations rather than pO_{2crit} thresholds, our results point towards plastic oxygen supply capacities to maintain sufficient oxygen provision (Seibel & Deutsch 2020), resulting in variable levels of absolute aerobic metabolic scope but not breadth or factorial aerobic scope. This, however, needs to be tested further (Deutsch et al. 2015, Scheuffele et al. 2021).

Data availability. All data required to produce the analyses in this study are included in the supplementary material.

Acknowledgements. We thank Monterey Abalone Company and Point Loma Marine Labs for supplying *S. purpuratus* specimens; Stanford University's Hopkins Marine Station and University of Washington's Friday Harbor Labs for laboratory space; the Monterey Bay Aquarium and Laura Rogers-Bennet for access to oceanographic data; Jason Hodin for advice regarding spawning and rearing *S. purpuratus*; Auston Rutledge for assistance with larval rearing; and Tom Levy for assistance with larvae counting. E.A.S. thanks Kevin Peterson and Richard Strathmann for inspiration and discussions on larval biology. Permission to collect wild urchins and conduct experiments at Friday Harbor Labs was granted by the Washington Department of Fish and Wildlife under permit number DUNCAN-20-171. This research was funded through an Environmental Venture Projects grant from the Stanford Woods Institute for the Environment at Stanford University awarded to E.A.S., C.J.L. and F.M., grants from the National Science Foundation (EAR-1922966) and the Paleontological Association (PA-RG201903) awarded to E.A.S., NSF DISES grant (2108566) awarded to F.M., and NOAA Saltonstall-Kennedy (#NA16-NMF4270255) and California Sea Grant (R/HCME-20B) awarded to S.L.H.

LITERATURE CITED

Alter K, Paschke K, Gebauer P, Cumillaf JP, Pörtner HO (2015) Differential physiological responses to oxygen availability in early life stages of decapods developing in distinct environments. Mar Biol 162:1111–1124

Alter K, Andrewartha SJ, Elliott NG (2016) Hatchery conditions do not negatively impact respiratory response of early life-stage development in Australian hybrid abalone. J Shellfish Res 35:585–591

Audzijonyte A, Richards SA, Stuart-Smith RD, Pecl G and others (2020) Fish body sizes change with temperature but not all species shrink with warming. Nat Ecol Evol 4: 809–814

Azad AK, Pearce CM, Mckinley RS (2012) Influence of stocking density and temperature on early development and survival of the purple sea urchin, *Strongylocentrotus purpuratus*. Aquacult Res 43:1577–1591

Birk MA (2020) respirometry: tools for conducting and analyzing respirometry experiments. R package version 1.2.1. https://doi.org/10.32614/CRAN.package.respirometry

Boag TH, Stockey RG, Elder LE, Hull PM, Sperling EA (2018) Oxygen, temperature and the deep-marine stenothermal cradle of Ediacaran evolution. Proc R Soc B 285:20181724

Borowiec BG, Crans KD, Khajali F, Pranckevicius NA, Young A, Scott GR (2016) Interspecific and environment-induced variation in hypoxia tolerance in sunfish. Comp Biochem Physiol A Mol Integr Physiol 198:59–71

Bozinovic F, Pörtner HO (2015) Physiological ecology meets climate change. Ecol Evol 5:1025–1030

Breitburg D, Levin LA, Oschlies A, Grégoire M and others (2018) Declining oxygen in the global ocean and coastal waters. Science 359:eaam7240

Brown JH, Gillooly JF, Allen AP, Savage VM, West GB (2004) Toward a metabolic theory of ecology. Ecology 85: 1771–1789

Chu JWF, Gale KSP (2017) Ecophysiological limits to aerobic metabolism in hypoxia determine epibenthic distributions and energy sequestration in the northeast Pacific Ocean. Limnol Oceanogr 62:59–74

Claireaux G, Chabot D (2016) Responses by fishes to environmental hypoxia: integration through Fry's concept of aerobic metabolic scope. J Fish Biol 88:232–251

Collins GM, Clark TD, Rummer JL, Carton AG (2013) Hypoxia tolerance is conserved across genetically distinct sub-populations of an iconic, tropical Australian teleost (*Lates calcarifer*). Conserv Physiol 1:cot029

Collins M, Truebano M, Verberk WCEP, Spicer JI (2021) Do aquatic ectotherms perform better under hypoxia after warm acclimation? J Exp Biol 224:jeb232512

Dahlke FT, Wohlrab S, Butzin M, Pörtner HO (2020) Thermal bottlenecks in the life cycle define climate vulnerability of fish. Science 369:65–70

Davidson EH, Rast JP, Oliveri P, Ransick A and others (2002) A genomic regulatory network for development. Science 295:1669–1678

Deutsch C, Ferrel A, Seibel B, Portner HO, Huey RB (2015) Climate change tightens a metabolic constraint on marine habitats. Science 348:1132–1135

Deutsch C, Penn JL, Seibel B (2020) Metabolic trait diversity shapes marine biogeography. Nature 585:557–562

Dolinar D, Edwards M (2021) The metabolic depression and revival of purple urchins (*Strongylocentrotus purpuratus*) in response to macroalgal availability. J Exp Mar Biol Ecol 545:151646

Donelson JM, Sunday JM, Figueira WF, Gaitán-Espitia JD and others (2019) Understanding interactions between plasticity, adaptation and range shifts in response to marine environmental change. Philos Trans R Soc B 374: 20180186

Duncan MI, James NC, Potts WM, Bates AE (2020) Different drivers, common mechanism; the distribution of a reef fish is restricted by local-scale oxygen and temperature constraints on aerobic metabolism. Conserv Physiol 8: coaa090

Duncan MI, Micheli F, Boag TH, Marquez JA, Deres H, Deutsch CA, Sperling EA (2023) Oxygen availability and body mass modulate ectotherm responses to ocean warming. Nat Commun 13:3811

Ebert TA (2010) Demographic patterns of the purple sea urchin *Strongylocentrotus purpuratus* along a latitudinal gradient, 1985–1987. Mar Ecol Prog Ser 406:105–120

Edworthy C, James NC, Erasmus B, Kemp JOG, Kaiser H, Potts WM (2018) Metabolic activity throughout early development of dusky kob *Argyrosomus japonicus* (Sciaenidae). Afr J Mar Sci 40:67–74

Eerkes-Medrano D, Menge BA, Sislak C, Langdon CJ (2013) Contrasting effects of hypoxic conditions on survivorship of planktonic larvae of rocky intertidal invertebrates. Mar Ecol Prog Ser 478:139–151

Endress MGA, Penn JL, Boag TH, Burford BP, Sperling EA, Deutsch CA (2024) Thermal optima in the hypoxia tolerance of marine ectotherms: physiological causes and biogeographic consequences. PLOS Biol 22:e3002443

Ern R, Johansen JL, Rummer JL, Esbaugh AJ (2017) Effects of hypoxia and ocean acidification on the upper thermal niche boundaries of coral reef fishes. Biol Lett 13:20170135

Frölicher TL, Fischer EM, Gruber N (2018) Marine heatwaves under global warming. Nature 560:360–364

Fulton EA (2011) Interesting times: winners, losers, and system shifts under climate change around Australia. ICES J Mar Sci 68:1329–1342

Gillooly JF, Brown JH, West GB, Savage VM, Charnov EL (2001) Effects of size and temperature on metabolic rate. Science 293:2248–2251

Han P, Bartels DM (1996) Temperature dependence of oxygen diffusion in H_2O and D_2O. J Phys Chem 100: 5597–5602

Hancock JR, Place SP (2016) Impact of ocean acidification on the hypoxia tolerance of the woolly sculpin, *Clinocottus analis.* Conserv Physiol 4:cow040

Harianto J, Carey N, Byrne M (2019) RespR — an R package for the manipulation and analysis of respirometry data. Methods Ecol Evol 10:912–920

Hendler G (2013) Recent mass mortality of *Strongylocentrotus purpuratus* (Echinodermata: Echinoidea) at Malibu and a review of purple sea urchin kills elsewhere in California. Bull South Calif Acad Sci 112:19–37

Heyland A, Hodin J (2014) A detailed staging scheme for late larval development in *Strongylocentrotus purpuratus* focused on readily-visible juvenile structures within the rudiment. BMC Dev Biol 14:22

Hilton Z, Wellenreuther M, Clements KD (2008) Physiology underpins habitat partitioning in a sympatric sister-species pair of intertidal fishes. Funct Ecol 22:1108–1117

Hinegardner RT (1969) Growth and development of the laboratory cultured sea urchin. Biol Bull (Woods Hole) 137: 465–475

Hodin J, Heyland A, Mercier A, Pernet B and others (2019) Culturing echinoderm larvae through metamorphosis. Methods Cell Biol 150:125–169

Hoegh-Guldberg O, Pearse JS (1995) Temperature, food availability, and the development of marine invertebrate larvae. Am Zool 35:415–425

Howard EM, Frenzel H, Kessouri F, Renault L, Bianchi D, McWilliams JC, Deutsch C (2020a) Attributing causes of future climate change in the California Current System with multimodel downscaling. Global Biogeochem Cycles 34:e2020GB00664

Howard EM, Penn JL, Frenzel H, Seibel BA and others (2020b) Climate-driven aerobic habitat loss in the California Current System. Sci Adv 6:eaay3188

Jacox MG, Alexander MA, Stock CA, Hervieux G (2019) On the skill of seasonal sea surface temperature forecasts in the California Current System and its connection to ENSO variability. Clim Dyn 53:7519–7533

Jensen RR, Benfey TJ (2022) Acclimation to warmer temperature reversibly improves high-temperature hypoxia tolerance in both diploid and triploid brook charr, *Salvelinus fontinalis.* Comp Biochem Physiol A Mol Integr Physiol 264:111099

Jurgens LJ, Rogers-Bennett L, Raimondi PT, Schiebelhut LM, Dawson MN, Grosberg RK, Gaylord B (2015) Patterns of mass mortality among rocky shore invertebrates across 100 km of Northeastern Pacific coastline. PLOS ONE 10:e0126280

Kaschner K, Kesner-Reyes K, Garilao C, Segschneider J, Rius-Barile J, Rees T, Froese R (2019) AquaMaps: predicted range maps for aquatic species. https://www.aquamaps.org

Killen SS, Christensen EAF, Cortese D, Závorka L and others (2021) Guidelines for reporting methods to estimate metabolic rates by aquatic intermittent-flow respirometry. J Exp Biol 224:jeb242522

Lavender E, Fox CJ, Burrows MT (2021) Modelling the impacts of climate change on thermal habitat suitability for shallow-water marine fish at a global scale. PLOS ONE 16:e0258184

Layous M, Khalaily L, Gildor T, de-Leon SBT (2021) The tolerance to hypoxia is defined by a time-sensitive response of the gene regulatory network in sea urchin embryos. Development 148:dev195859

Leung JYS, Russell BD, Coleman MA, Kelaher BP, Connell SD (2021) Long-term thermal acclimation drives adaptive physiological adjustments of a marine gastropod to reduce sensitivity to climate change. Sci Total Environ 771: 145208

Low NHN, Micheli F (2018) Lethal and functional thresholds of hypoxia in two key benthic grazers. Mar Ecol Prog Ser 594:165–173

Low NHN, Micheli F (2020) Short- and long-term impacts of variable hypoxia exposures on kelp forest sea urchins. Sci Rep 10:2632

Low NHN, Micheli F, Domingo Aguilar J, Romero Arce D and others (2021) Variable coastal hypoxia exposure and drivers across the southern California Current. Sci Rep 11:10929

Lowe CJ, Wray GA (2000) Rearing larvae of sea urchins and sea stars for developmental studies. Methods Mol Biol 135:9–15

MacCready P, McCabe RM, Siedlecki SA, Lorenz M and others (2021) Estuarine circulation, mixing, and residence times in the Salish Sea. J Geophys Res Oceans 126:e2020JC016738

Madliger CL, Franklin CE, Hultine KR, van Kleunen M and others (2017) Conservation physiology and the quest for a 'good' Anthropocene. Conserv Physiol 5:cox003

Marsh AG, Manahan DT (1999) A method for accurate measurements of the respiration rates of marine invertebrate embryos and larvae. Mar Ecol Prog Ser 184:1–10

Martin BT, Dudley PN, Kashef NS, Stafford DM and others (2020) The biophysical basis of thermal tolerance in fish eggs. Proc R Soc B 287:20201550

McBryan TL, Healy TM, Haakons KL, Schulte PM (2016) Warm acclimation improves hypoxia tolerance in *Fundulus heteroclitus.* J Exp Biol 219:474–484

McEdward LR, Miner BG (2001) Larval and life-cycle patterns in echinoderms. Can J Zool 79:1125–1170

McKenzie DJ, Lund I, Pedersen PB (2008) Essential fatty acids influence metabolic rate and tolerance of hypoxia in Dover sole (*Solea solea*) larvae and juveniles. Mar Biol 154:1041–1051

Meyer E, Green AJ, Moore M, Manahan DT (2007) Food availability and physiological state of sea urchin larvae (*Strongylocentrotus purpuratus*). Mar Biol 152:179–191

Ng CA, Micheli F (2020) Short-term effects of hypoxia are more important than effects of ocean acidification on grazing interactions with juvenile giant kelp (*Macrocystis pyrifera*). Sci Rep 10:5403

Nilsson GE, Östlund-Nilsson S, Penfold R, Grutter AS (2007) From record performance to hypoxia tolerance: respiratory transition in damselfish larvae settling on a coral reef. Proc R Soc B 274:79–85

Nilsson GE, Östlund-Nilsson S, Munday PL (2010) Effects of elevated temperature on coral reef fishes: loss of hypoxia tolerance and inability to acclimate. Comp Biochem Physiol A Mol Integr Physiol 156:389–393

Nilsson-Örtman V, Brönmark C (2022) The time course of metabolic plasticity and its consequences for growth performance under variable food supply in the northern pike. Proc R Soc B 289:20220427

Okamoto DK, Schroeter SC, Reed DC (2020) Effects of ocean climate on spatiotemporal variation in sea urchin settlement and recruitment. Limnol Oceanogr 65:2076–2091

Pearse JS (2006) Ecological role of purple sea urchins. Science 314:940–941

Pearse JS, Cameron RA (1991) Echinodermata: Echinoidea. In: Giese AC, Pearse JS, Pearse VB (eds) Reproduction of marine invertebrates. Vol 6: Echinoderms and lophophorates. Boxwood Press, Pacific Grove, CA, p 513–662

Peck MA, Moyano M (2016) Measuring respiration rates in marine fish larvae: challenges and advances. J Fish Biol 88:173–205

Penn JL, Deutsch C, Payne JL, Sperling EA (2018) Temperature-dependent hypoxia explains biogeography and severity of end-Permian marine mass extinction. Science 362:eaat1327

Poloczanska ES, Brown CJ, Sydeman WJ, Kiessling W and others (2013) Global imprint of climate change on marine life. Nat Clim Change 3:919–925

Reddin CJ, Nätscher PS, Kocsis ÁT, Pörtner HO, Kiessling W (2020) Marine clade sensitivities to climate change conform across timescales. Nat Clim Change 10: 249–253

Regan MD, Mandic M, Dhillon RS, Lau GY and others (2019) Don't throw the fish out with the respirometry water. J Exp Biol 222:jeb200253

Renault L, McWilliams JC, Kessouri F, Jousse A, Frenzel H, Chen R, Deutsch C (2021) Evaluation of high-resolution atmospheric and oceanic simulations of the California Current System. Prog Oceanogr 195:102564

Rijnsdorp AD, Peck MA, Engelhard GH, Mollmann C, Pinnegar JK (2009) Resolving the effect of climate change on fish populations. ICES J Mar Sci 66:1570–1583

Roegner GC, Needoba JA, Baptista AM (2011) Coastal upwelling supplies oxygen-depleted water to the Columbia River estuary. PLOS ONE 6:e18672

Rogers NJ, Urbina MA, Reardon EE, McKenzie DJ, Wilson RW (2016) A new analysis of hypoxia tolerance in fishes using a database of critical oxygen level (P_{crit}). Conserv Physiol 4:cow012

Rogers-Bennett L (2013) *Strongylocentrotus franciscanus* and *Strongylocentrotus purpuratus*. In: Lawrence JM (ed) Sea urchins: biology and ecology, 3rd edn. Developments in Aquaculture and Fisheries Science, Vol 38. Elsevier, Oxford, p 413–435

Rogers-Bennett L, Catton CA (2019) Marine heat wave and multiple stressors tip bull kelp forest to sea urchin barrens. Sci Rep 9:15050

Rogers-Bennett L, Okamoto D (2020) *Mesocentrotus franciscanus* and *Strongylocentrotus purpuratus*. In: Lawrence JM (ed) Sea urchins: biology and ecology. Developments in Aquaculture and Fisheries Science, Vol 43. Elsevier, Oxford, p 593–608

Roman MR, Brandt SB, Houde ED, Pierson JJ (2019) Interactive effects of hypoxia and temperature on coastal pelagic zooplankton and fish. Front Mar Sci 6:139

Rosa R, Trübenbach K, Repolho T, Pimentel M and others (2013) Lower hypoxia thresholds of cuttlefish early life stages living in a warm acidified ocean. Proc R Soc B 280: 20131695

Sampaio E, Santos C, Rosa IC, Ferreira V and others (2021) Impacts of hypoxic events surpass those of future ocean warming and acidification. Nat Ecol Evol 5:311–321

Scheuffele H, Rubio-Gracia F, Clark TD (2021) Thermal performance curves for aerobic scope in a tropical fish (*Lates calcarifer*): flexible in amplitude but not breadth. J Exp Biol 224:243504

Schulte PM (2015) The effects of temperature on aerobic metabolism: towards a mechanistic understanding of the responses of ectotherms to a changing environment. J Exp Biol 218:1856–1866

Seebacher F, White CR, Franklin CE (2015) Physiological plasticity increases resilience of ectothermic animals to climate change. Nat Clim Change 5:61–66

Seibel BA, Deutsch C (2020) Oxygen supply capacity in animals evolves to meet maximum demand at the current oxygen partial pressure regardless of size or temperature. J Exp Biol 223:jeb210492

Seibel BA, Andres A, Birk MA, Burns AL, Shaw CT, Timpe AW, Welsh CJ (2021) Oxygen supply capacity breathes new life into critical oxygen partial pressure (P_{crit}). J Exp Biol 224:jeb242210

Sinclair BJ, Marshall KE, Sewell MA, Levesque DL and others (2016) Can we predict ectotherm responses to climate change using thermal performance curves and body temperatures? Ecol Lett 19:1372–1385

Slesinger E, Andres A, Young R, Seibel B and others (2019) The effect of ocean warming on black sea bass (*Centropristis striata*) aerobic scope and hypoxia tolerance. PLOS ONE 14:e0218390

Smith MM, Smith LC, Cameron RA, Urry LA (2008) The larval stages of the sea urchin, *Strongylocentrotus purpuratus.* J Morphol 269:713–733

Snyder S, Nadler LE, Bayley JS, Svendsen MBS, Johansen JL, Domenici P, Steffensen JF (2016) Effect of closed v. intermittent-flow respirometry on hypoxia tolerance in the shiner perch *Cymatogaster aggregata.* J Fish Biol 88: 252–264

Sodergren E, Weinstock GM, Davidson EH, Cameron RA and others (2006) The genome of the sea urchin *Strongylocentrotus purpuratus.* Science 314:941–952

Somero GN (2010) The physiology of climate change: how potentials for acclimatization and genetic adaptation will determine 'winners' and 'losers'. J Exp Biol 213:912–920

Sørensen C, Munday PL, Nilsson GE (2014) Aerobic vs. anaerobic scope: sibling species of fish indicate that temperature dependence of hypoxia tolerance can predict future survival. Glob Change Biol 20:724–729

Sperling EA, Knoll AH, Girguis PR (2015) The ecological physiology of earth's second oxygen revolution. Annu Rev Ecol Evol Syst 46:215–235

Strathmann RR (1971) The feeding behavior of planktotrophic echinoderm larvae: mechanisms, regulation, and rates of suspension feeding. J Exp Mar Biol Ecol 6:109–160

Strathmann MF (1987) Reproduction and development of marine invertebrates of the northern Pacific coast: data and methods for the study of eggs, embryos, and larvae. University of Washington Press, Seattle, WA

Svendsen MBS, Bushnell PG, Steffensen JF (2016) Design and setup of intermittent-flow respirometry system for aquatic organisms. J Fish Biol 88:26–50

Ultsch GR, Regan MD (2019) The utility and determination of P_{crit} in fishes. J Exp Biol 222:jeb203646

Vaquer-Sunyer R, Duarte CM (2008) Thresholds of hypoxia for marine biodiversity. Proc Natl Acad Sci USA 105: 15452–15457

Vargo SL, Sastry AN (1977) Acute temperature and low dissolved oxygen tolerances of brachyuran crab (*Cancer irroratus*) larvae. Mar Biol 40:165–171

Wood CM (2018) The fallacy of the P_{crit} – Are there more useful alternatives? J Exp Biol 221:jeb163717

Editorial responsibility: James McClintock, Birmingham, Alabama, USA
Reviewed by: M. Birk and 2 anonymous referees

Submitted: November 27, 2023
Accepted: April 22, 2024
Proofs received from author(s): June 28, 2024